Supporting Information for:

Redox-active ligand assisted electrocatalytic water oxidation by a mononuclear cobalt complex

Sachidulal Biswas,[1] Suranjana Bose,[2] Joyashish Debgupta,*[,3] Purak Das [4] and Achintesh N. Biswas*[,1]

[1] Department of Chemistry, National Institute of Technology Sikkim, Ravangla, South Sikkim 737139, India

[2] Green Chemistry Centre of Excellence, Department of Chemistry, University of York, York YO10 5DD, UK

[3] Department of Chemistry, University of York, York YO10 5DD, UK

[4] Department of Chemistry, Rishi Bankim Chandra College for Women, Naihati 743165, India

Table of Contents

Sample preparation for SEM and EDX experiment

The FTO surface was cleaned with deionised water prior to SEM and EDX analysis. The FTO electrode was then used for CPE and then again washed with deionised water and dried. The dried FTO was then analysed by SEM and EDX.

Calibration of Ag/AgCl with respect to NHE

The Ag/AgCl reference electrode was calibrated using linear sweep voltammetry technique. The LSV was taken using a Pt-disk (2 mm diameter) in H_2 saturated 0.1M phosphate buffer (pH 8) at a scan rate of 1 mV/sec using the Ag/AgCl (satd KCl) reference electrode in the potential region 0 to -1 V. The potential where the voltammogram crosses 0 (zero) current was considered the potential of the Ag/AgCl *vs* RHE.[1]

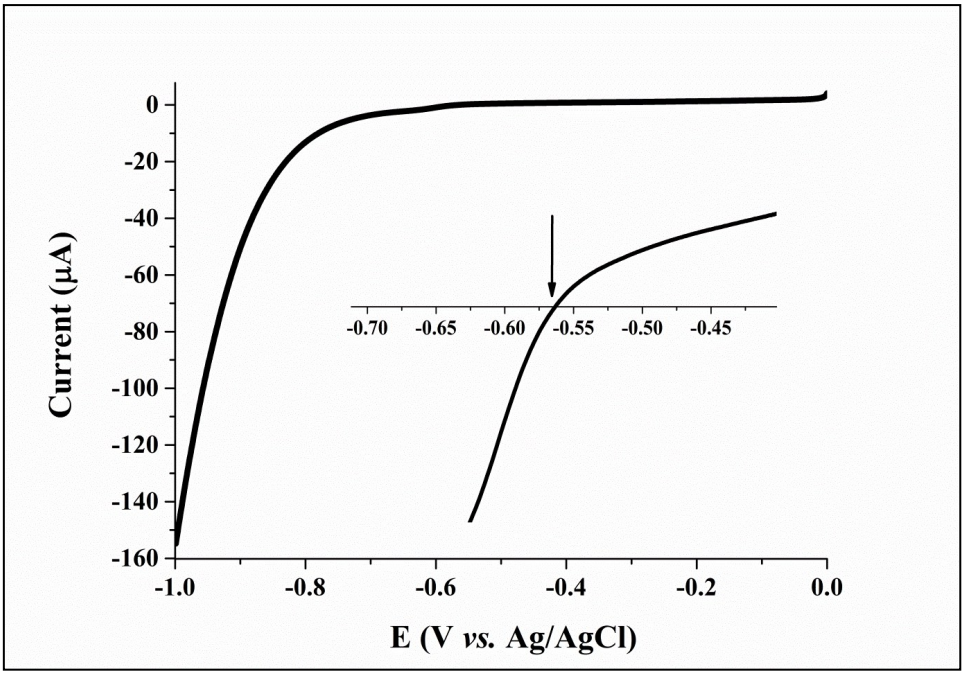

Figure S1: LSV plot for Ag/AgCl reference electrode calibration. Pt-disk was used as working electrode, Pt wire as counter electrode and Ag/AgCl as reference electrode in H_2-saturated 0.1 M phosphate buffer (pH 8) solution using scan rate of 1 mV/s.

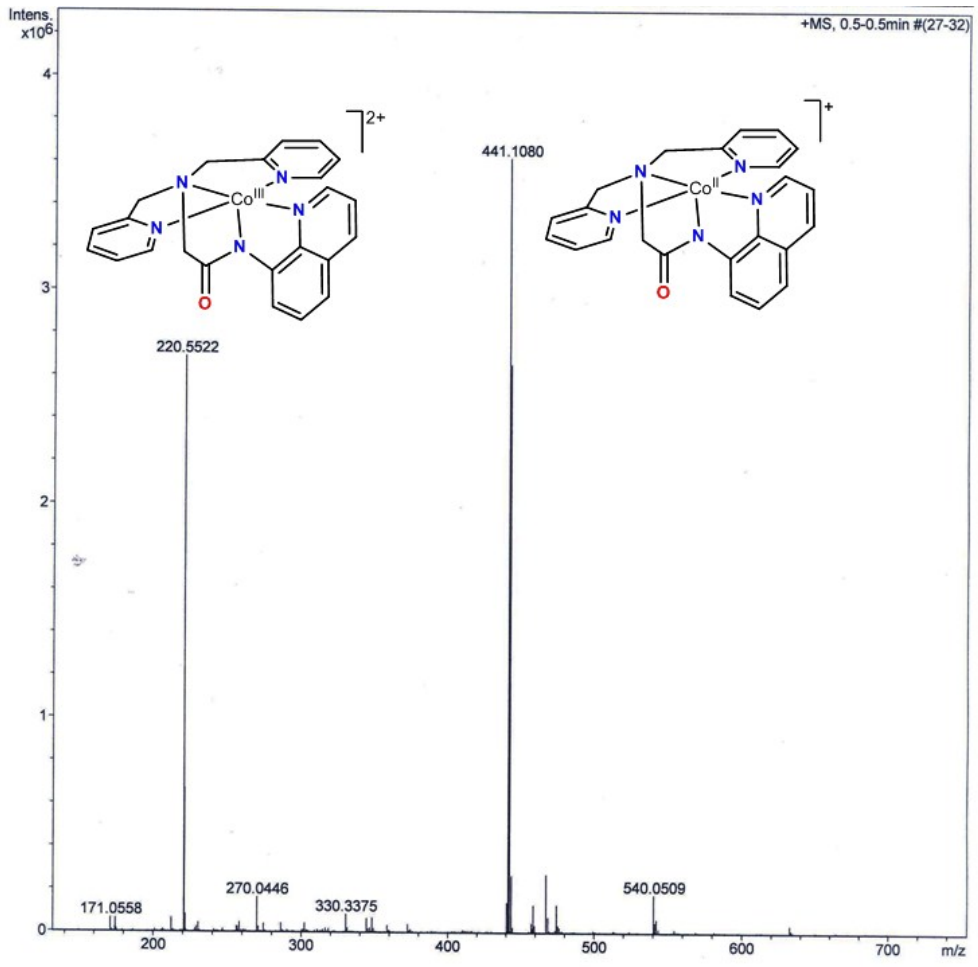

Figure S2: ESI-MS spectra of complex $\mathbf{[1^{II}1^{III}].3ClO_4}$ in acetonitrile.

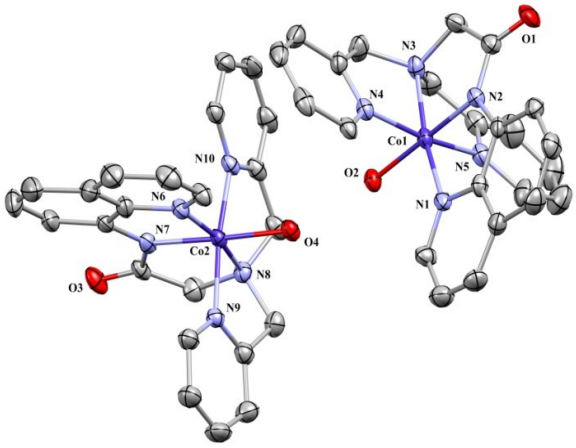

Figure S3: ORTEP representations of the two Co units, $[Co^{II}(dpaq)(H_2O)]^+$, $\mathbf{[1^{II}]^+}$ and $[Co^{III}(dpaq)(H_2O)]^{2+}$, $\mathbf{[1^{III}]^{2+}}$ (ellipsoids were drawn at 30% probability and the counter anions, hydrogens were omitted for clarity). Full crystallographic details are given in Table S1 and Table S2.

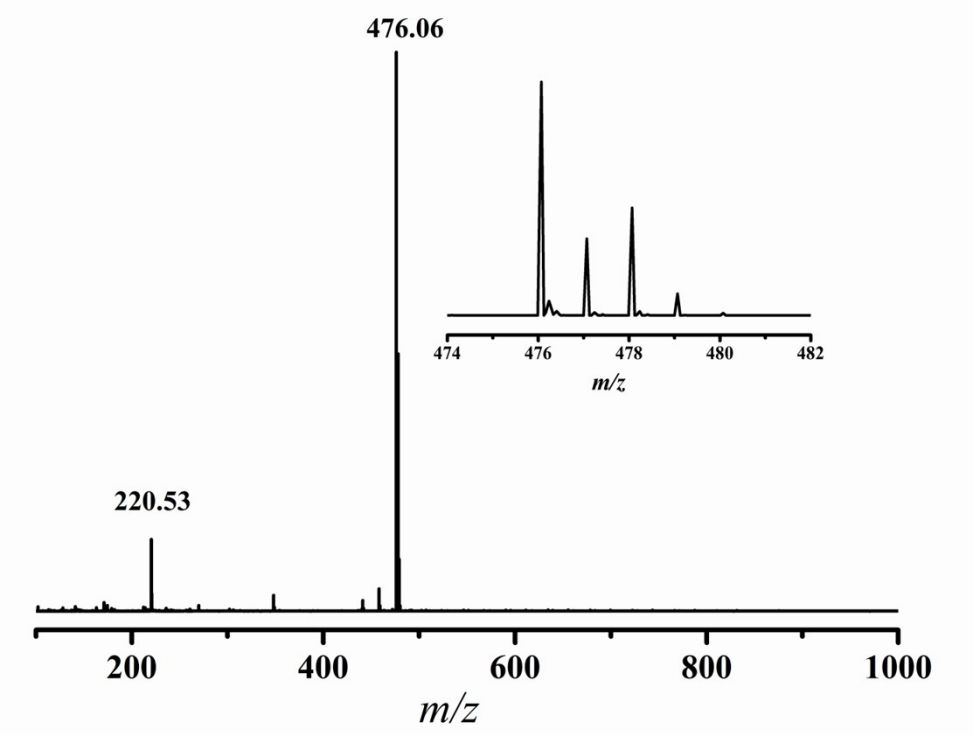

Figure S4: ESI-MS spectra of complex **1** in water.

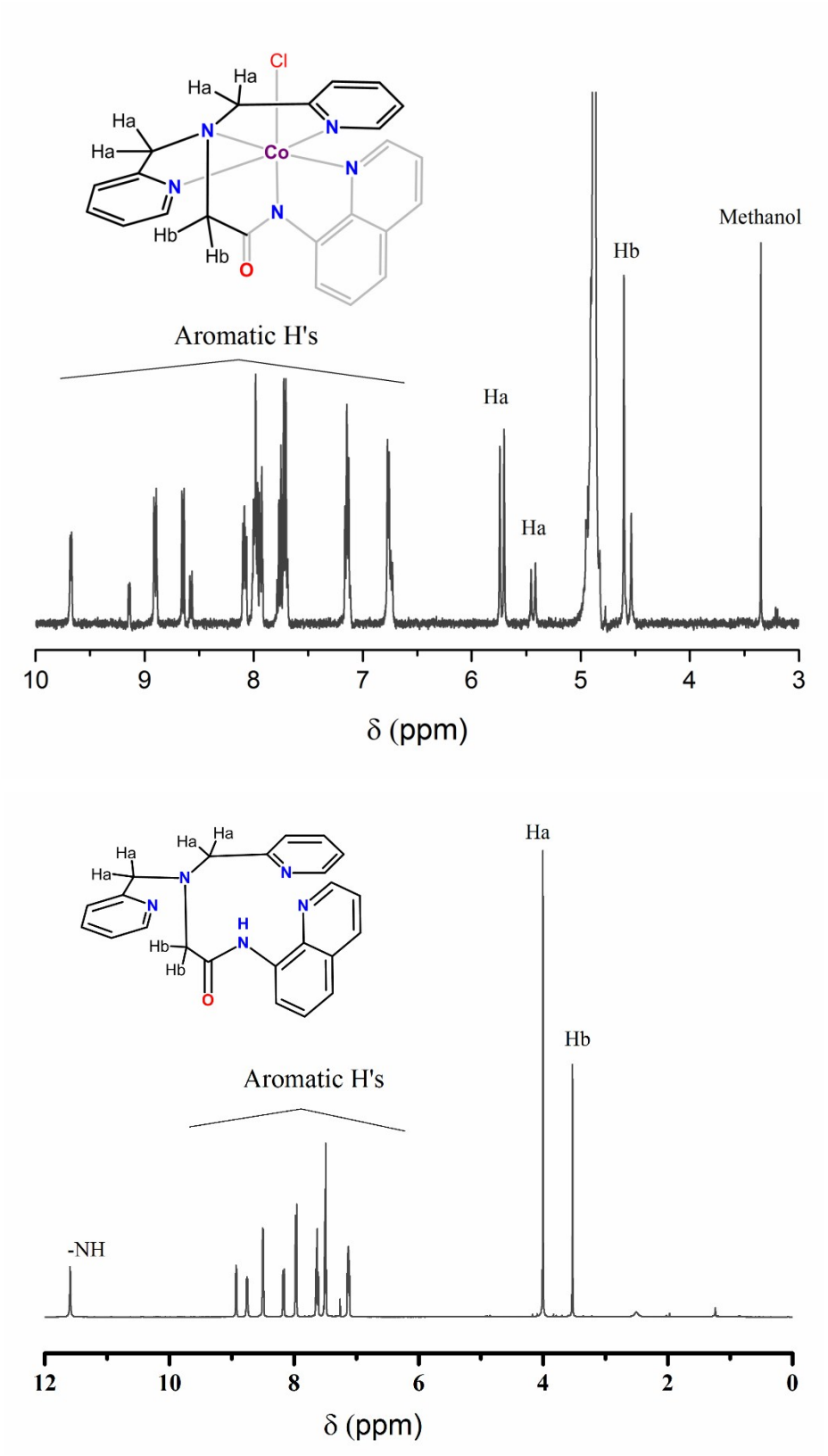

Figure S5: ^{1}H NMR spectrum of the complex **1** in D_2O (top) and H-dpaq in $CDCl_3$ (bottom) using a Bruker 400 MHz spectrometer.

Table S1 Crystal data collection and structure refinement for **$[1^{II}1^{III}].3ClO_4$**

Crystal data	
CCDC reference number	CCDC-1573631
Empirical formula	$Co_2C_{46}H_{47}N_{10}O_{17}Cl_3$
Moiety formula	$CoC_{23}H_{23}N_5O_2$, $CoC_{23}H_{22}N_5O_2$, $3(ClO_4)$, H_2O
Formula weight	1236.15
Crystal system	Monoclinic
Space group	P 21/c
Colour, habit	Purple, rod
Size, mm	0.22 × 0.18 × 0.16
Unit cell dimensions	
	a = 12.563(5)Å α = 90°
	b = 18.556(8)Å β = 94.530(6)°
	c = 23.167(10)Å γ = 90°
Volume Å^3	5384(4)
Z	4
Density (calculated), Mg/m^3	1.525
Absorption coefficient, mm^{-1}	0.844
F(000)	2536
Data collection	
Temperature, K	293(2)
Theta range for data collection	1.96° to 25.58°
Index ranges	$-13 \le h \le 15$
	$-22 \le k \le 22$
	$-23 \le l \le 28$
Reflections collected	25953
Unique reflections	9816
Observed reflections (>2σ*(I)*)	5566
R_{int}	0.0765
Completeness to θ, %	25.58°, 97.2
Absorption correction	Multi-scan (SADABS; Bruker, 2000)
	T_{min} = 0.834, T_{max} = 0.873
Refinement	
Refinement method	Full-matrix least-squares on F^2
Data / restraints / parameters	9816 / 1 / 711
Calculated weights, *w*	$1/[\sigma^2(F_o^2) + (0.1592P)^2 + 0.0000P]$ where $P = (F_o^2 + 2F_c^2)/3$
Goodness-of-fit on F^2	1.018
Final R indices [I > 2σ(I)]	R_1 = 0.0873, wR_2 = 0.2292
R indices (all data)	R_1 = 0.1482, wR_2 = 0.2688
Largest diff. peak and hole	1.642 and -0.865 e.Å^{-3}

Table S2 Selected bond lengths (Å), bond angles (°) and torsion angles (°) for **$[1^{II}1^{III}].3ClO_4$**

Bond lengths (Å)			
Co(1)–O(2)	1.937(4)	Co(2)–O(4)	1.920(4)
Co(1)–N(1)	1.924(6)	Co(2)–N(6)	1.941(5)
Co(1)–N(2)	1.879(5)	Co(2)–N(7)	1.885(5)
Co(1)–N(3)	1.952(6)	Co(2)–N(8)	1.942(5)
Co(1)–N(4)	1.939(5)	Co(2)–N(9)	1.936(5)
Co(1)–N(5)	1.944(5)	Co(2)–N(10)	1.939(5)
N(2)–C(10)	1.369(8)	N(7)–C(33)	1.325(8)
O(1)–C(10)	1.224(7)	O(3)–C(33)	1.259(7)
Bond angles (°)			
O(2)–Co(1)–N(1)	96.3(2)	O(4)–Co(2)–N(6)	95.1(2)
O(2)–Co(1)–N(3)	93.2(2)	O(4)–Co(2)–N(8)	95.3(2)
O(2)–Co(1)–N(4)	88.94(19)	O(4)–Co(2)–N(9)	90.5(2)
O(2)–Co(1)–N(5)	89.2(2)	O(4)–Co(2)–N(10)	87.06(19)
N(2)–Co(1)–N(1)	84.0(2)	N(7)–Co(2)–N(6)	84.2(2)
N(2)–Co(1)–N(3)	86.5(2)	N(7)–Co(2)–N(8)	85.4(2)
N(2)–Co(1)–N(4)	91.3(2)	N(7)–Co(2)–N(9)	91.6(2)
N(2)–Co(1)–N(5)	90.5(2)	N(7)–Co(2)–N(10)	91.0(2)
N(1)–Co(1)–N(4)	95.7(2)	N(6)–Co(2)–N(9)	94.1(2)
N(1)–Co(1)–N(5)	96.1(2)	N(6)–Co(2)–N(10)	96.9(2)
N(3)–Co(1)–N(4)	84.8(2)	N(8)–Co(2)–N(9)	83.7(2)
N(3)–Co(1)–N(5)	83.6(2)	N(8)–Co(2)–N(10)	85.7(2)

Table S3 Crystal data collection and structure refinement for **1**

Crystal data	
CCDC reference number	CCDC-1573631
Empirical formula	$CoC_{26}H_{32}N_5O_4Cl_2$
Moiety formula	$CoC_{23}H_{20}N_5OCl$, Cl, [+3(CH_3OH)]
Formula weight	608.40
Crystal system	Triclinic
Space group	P -1
Colour, habit	Clear dark brown, Plate
Size, mm	0.22 × 0.11 × 0.05
Unit cell dimensions	
a = 8.7167(6)Å	α = 112.930(7)°
b = 13.2069(8)Å	β = 92.528(7)°
c = 13.7214(12)Å	γ = 108.905(6)°
Volume Å^3	1349.76(17)
Z	2
Density (calculated), Mg/m^3	1.260
Absorption coefficient, mm^{-1}	0.855
F(000)	524
Data collection	
Temperature, K	293(2)
Theta range for data collection	3.00° to 25.00°
Index ranges	$-10 \le h \le 10$ $-15 \le k \le 15$ $-12 \le l \le 16$
Reflections collected	7284
Unique reflections	4725
Observed reflections (>2σ*(I)*)	3277
R_{int}	0.0935
Completeness to θ, %	25.00°, 99.4
Absorption correction	Multi-scan T_{min} = 0.891, T_{max} = 0.957
Refinement	
Refinement method	Full-matrix least-squares on F^2
Data / restraints / parameters	4725 / 0 / 290
Calculated weights, *w*	$1/[\sigma^2(F_o^2) + (0.1260P)^2 + 0.0000P]$ where $P = (F_o^2 + 2F_c^2)/3$
Goodness-of-fit on F^2	1.009
Final R indices [I > 2σ(I)]	R_1 = 0.0899, wR_2 = 0.2221
R indices (all data)	R_1 = 0.1057, wR_2 = 0.2417
Largest diff. peak and hole	0.870 and -1.004 e.Å^{-3}

Table S4 Selected bond lengths (Å), bond angles (°) and torsion angles (°) for **1.**

Bond lengths (Å)			
Co(1)–Cl(1)	2.2668(13)	Co(1)–N(3)	1.947(4)
Co(1)–N(1)	1.931(4)	Co(1)–N(4)	1.962(4)
Co(1)–N(2)	1.895(4)	Co(1)–N(5)	1.950(4)
Bond angles (°)			
Cl(1)–Co(1)–N(1)	94.41(12)	N(2)–Co(1)–N(4)	89.59(17)
Cl(1)–Co(1)–N(3)	95.04(12)	N(2)–Co(1)–N(5)	90.21(17)
Cl(1)–Co(1)–N(4)	88.99(11)	N(1)–Co(1)–N(4)	96.48(18)
Cl(1)–Co(1)–N(5)	91.56(12)	N(1)–Co(1)–N(5)	95.5(2)
N(2)–Co(1)–N(1)	84.00(16)	N(3)–Co(1)–N(4)	84.11(19)
N(2)–Co(1)–N(3)	86.56(17)	N(3)–Co(1)–N(5)	83.9(2)

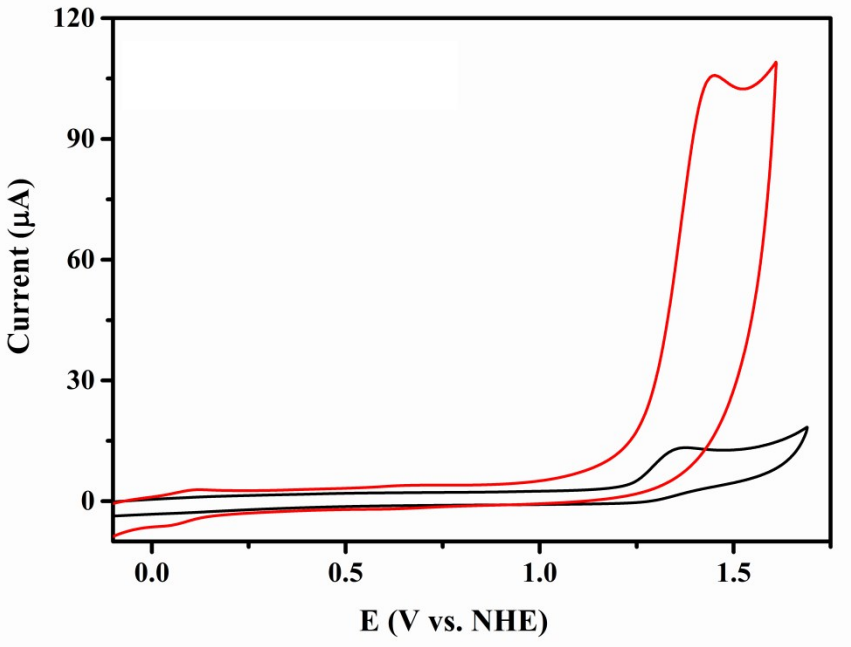

Figure S6: CV of complex **1** (0.5mM) (Red) and $[Zn(dpaq)]^+$ (0.5 mM) (Black) in 0.1 M phosphate buffer (pH=8) at a scan rate of 100 mVs^{-1} using a GC working electrode.

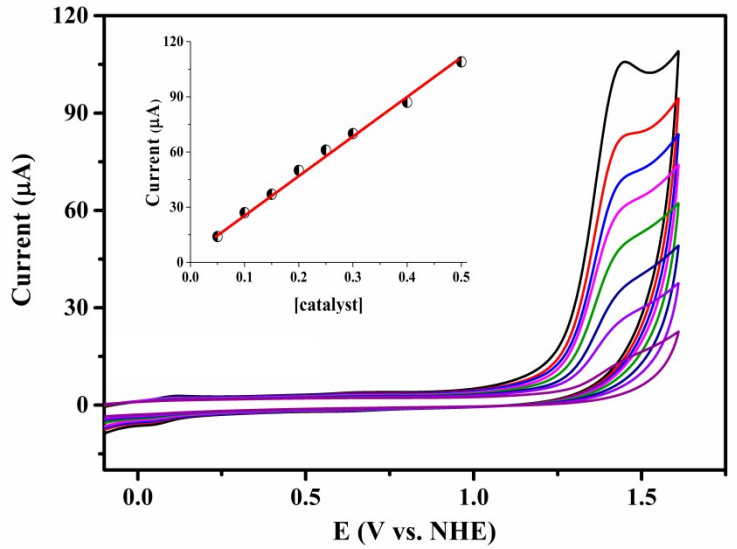

Figure S7: CV of complex **1** in 0.1 M phosphate buffer (pH=8) having different concentration (0.05mM purple, 0.1mM violet line, 0.15mM navy line, 0.2mM green line, 0.25mM magenta line, 0.3mM blue line, 0.4mM red line and 0.5mM black line) at a scan rate of 100 mVs^{-1} using a GC working electrode. Inset shows the plot of catalytic peak current (1.45 V) vs [catalyst].

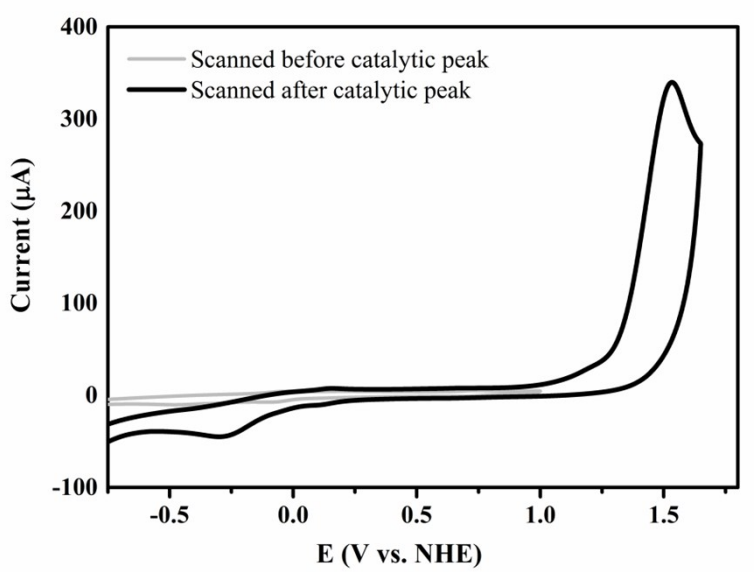

Figure S8: (top) Formation of oxygen indicated by the appearance of oxygen bubbles at the GC electrode surface. (bottom). CV of complex **1** (1.0 mM) in pH 8 0.1 M phosphate buffer recorded after multiple anodic scans when bubbles appeared at the electrode surface (black line). After the oxidative scans potential was reversed towards cathodic potentials where a broad reductive wave at -0.33 V (*vs.* NHE) appeared showing the reduction of oxygen. When the same was done before going to the catalytic wave no such reductive wave can be seen (grey line). This indicates the generation of oxygen due to water oxidation catalyzed by complex **1**. Glassy carbon working electrode, scan rate 100 mVs^{-1}.

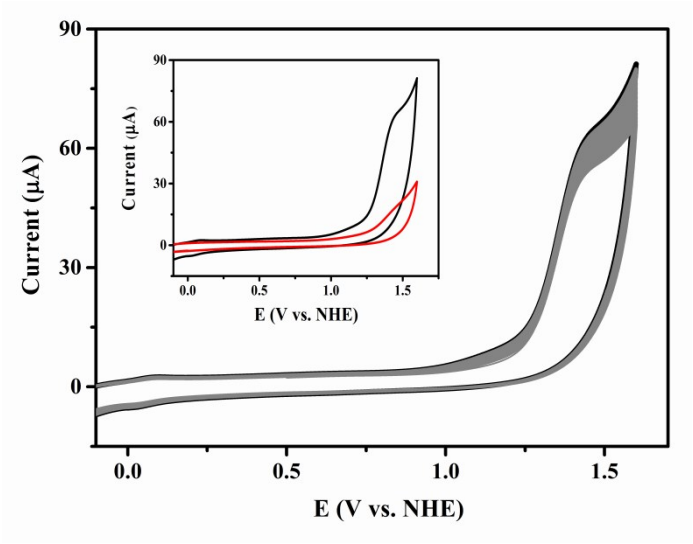

Figure S9: 15 consecutive CV cycles of complex **1** (0.3mM) in pH 8 0.1 M phosphate buffer and the inset shows the first CV cycle of the multiple scan (black line) and CV of the same electrode in blank buffer medium after 15 scans which was rinsed with water but not polished.

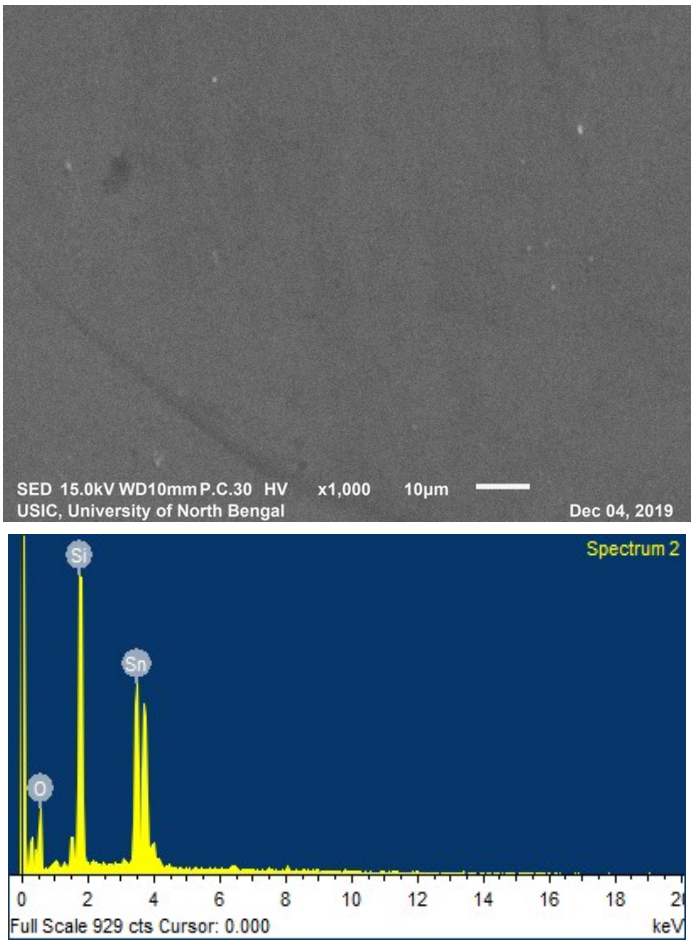

Figure S10: SEM image and EDX spectra of the FTO electrode used in CPE experiment after 3 hours of electrolysis.

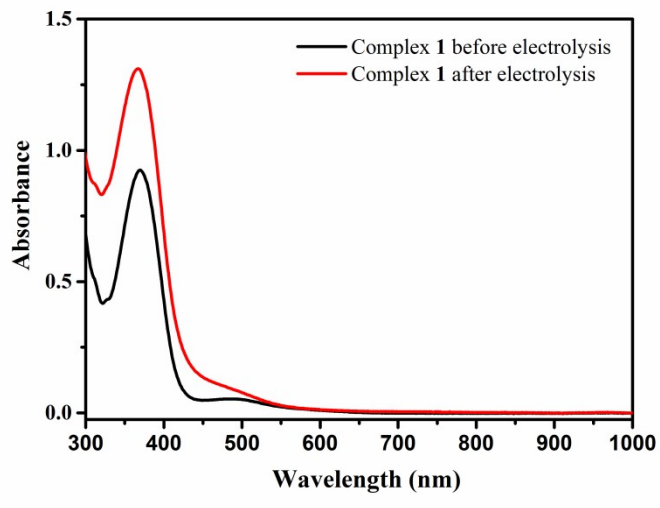

Figure S11: UV visible spectra of complex **1** (0.2 mM) before (black line) and after (red line) control potential electrolysis.

Electrochemical kinetic analysis by FOWA

CVs at different scan rate as well as at different catalyst concentrations were used to determine the kinetic parameters for water oxidation. We have applied FOWA methodology for the WNA and I2M mechanisms, for kinetic analysis using the following two equations[2],

For WNA

$$i \Big/ ip = \frac{4 \times 2.24 \sqrt{\left(\frac{RT}{F\vartheta}\right) kWNA}}{1 + exp\{\left(\frac{F}{RT}\right)(E0 - E)\}}$$

For I2M

$$i/ip = \frac{4 \times 2.24 \sqrt{\left(\frac{RT}{F\vartheta}\right) kDC0Cat}}{[1 + \exp\left\{\left(\frac{F}{RT}\right)(E0 - E)\right\}]3/2}$$

And TOF was calculated using the following equation

$$TOF = \frac{kWNA}{1 + exp\{F(E0 - EH2O/O2 - \eta)\}}$$

Where, C^{o}_{cat} : initial bulk concentration of catalyst; E^{o}: standard potential for the $Co^{IV/V}$ couple; $E_{H2O/O2}$: standard potential of oxidation of water at the working pH; F: Faradaic constant; η: overpotential; i: CV current intensity; i_p: peak current intensity of one-electron redox process of the catalyst; k_1: apparent WNA rate constant ; k_{WNA}: apparent WNA pseudo-rate constant ($k_1[H_2O]$); k_D: apparent dimerization constant; R: gas constant; T: temperature.

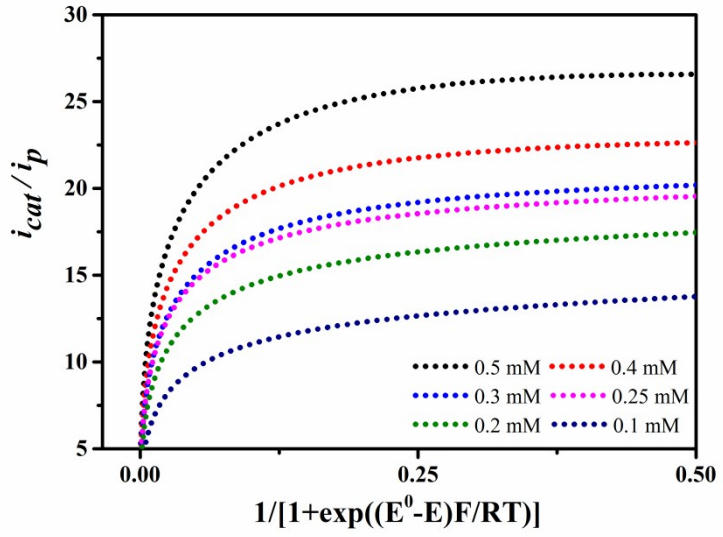

Figure S12: Plot of *i/ip* vs 1+exp{(*F/RT*)(*E*^{o}-*E*)} for foot of the wave analysis at different catalyst concentration.

Electrochemical kinetic analysis by following the classical Shain *et al.* methodology[3]

The linear dependency of catalytic peak current for water oxidation, i_{cat}, with the bulk concentration of the catalyst (Figure S7) is consistent with single-site cobalt catalysis and therefore, the peak current of the catalytic process should obey the following equation,

$$i_{cat} = n_{cat}FA[\mathbf{Co}](k_{cat}D_{\mathbf{1}})^{1/2} \qquad (1)$$

where i_{cat} is the peak current of the catalytic wave, n_{cat} = 4 is the number of electrons transferred in each catalytic cycle of water oxidation, A is the electrode surface area in cm^{-2}, F is the Faraday constant, [**Co**] is the bulk concentration of the catalyst (in mol/L), and $D_{\mathbf{1}}$ is the diffusion coefficient of the catalyst in 0.1 M phosphate buffer at pH 8. Moreover, as evident from Inset Figure S13, the peak current for the Co(III/IV) couple at 0.7 V *vs.* NHE varies linearly with the square root of the scan rate ($v^{1/2}$), which is consistent with the Randles-Sevcik equation,

$$i_d = 0.496n_dFA[\mathbf{Co}](n_dFvD_{\mathbf{1}}/RT)^{1/2} \qquad (2)$$

where, n_d = 1 is the number of electrons transferred in the diffusion controlled Co(III/IV) process and T is the absolute temperature. The ratio of Eq. 1 and 2 provides a relationship betweeni_{cat} and i_d (Eq. 3) allowing us to evaluate the rate constants for water oxidation.

$$i_{cat}/i_d = 0.359\ (n_{cat}/n_d)^{3/2}(k_{cat})^{1/2}(1/v^{1/2}) \qquad (3)$$

Thus, catalytic currents at 1.45 V *vs* NHE (i_{cat}) were normalized to the Co^{III}/Co^{IV}wave at 0.7 V (i_d) and i_{cat}/i_d was plotted against $v^{-1/2}$. From the slope of the plot of i_{cat}/i_p *vs* $v^{-1/2}$ (Figure S13), k_{cat} was calculated to be 85 s^{-1} in 0.1M phosphate buffer at pH 8.

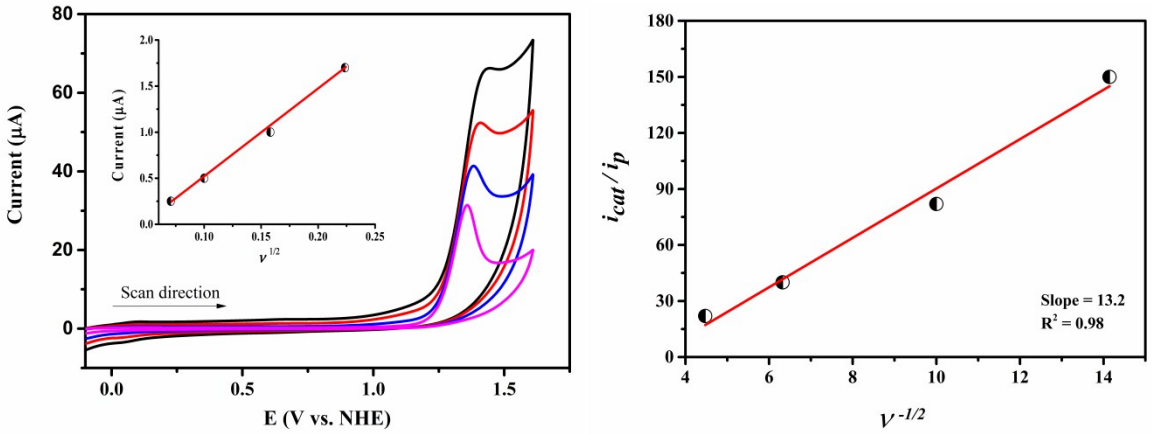

Figure S13: (left) Scan rate dependent CVs of **1** (0.5mM) in 0.1M phosphate buffer pH=8 using a GC working electrode, Pt counter electrode and Ag/AgCl reference electrode (black line 50mVs^{-1}, red line 25 mVs^{-1}, blue line 10 mVs^{-1} and pink line 5 mVs^{-1}). (inset) Plot of i_p *vs.* $v^{1/2}$ for electrocatalytic water oxidation in 0.1M phosphate buffer at pH=8 (black circles). (right) Background corrected plot of i_{cat}/i_p *vs* $1/v^{1/2}$ for electrocatalytic water oxidation in 0.1M phosphate buffer at pH=8 used for the determination of rate constant (black circles).

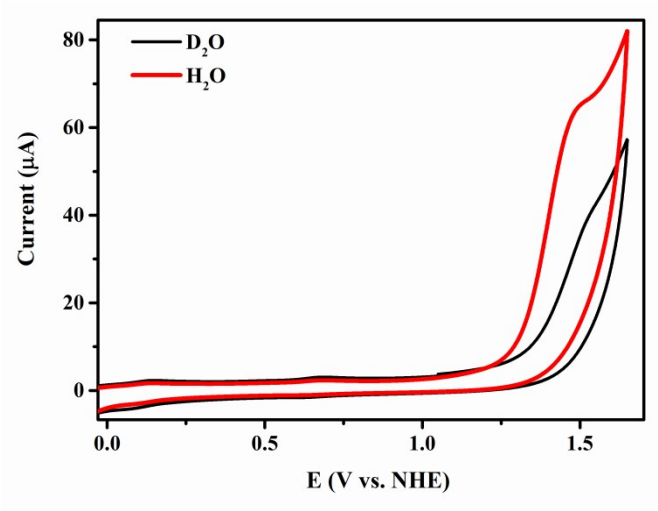

Figure S14: CV of complex **1** (0.3 mM) in pH 8 phosphate buffer (0.1 M) in H_2O (red line) and D_2O (black line) at GC working electrode. All the CVs were recorded at a scan rate of 100 mVs^{-1}.

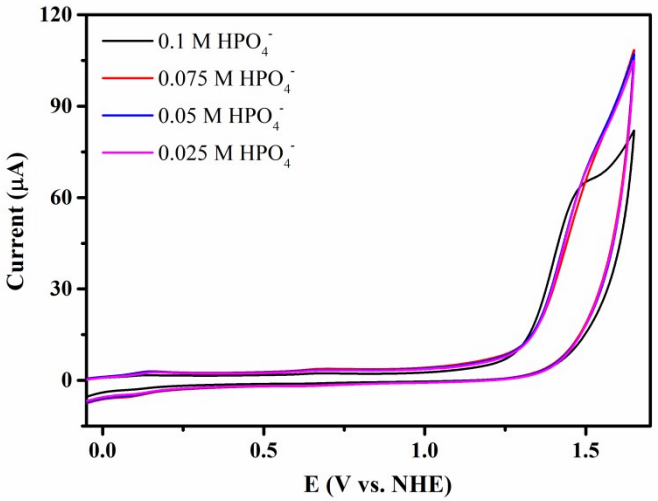

Figure S15: CV of complex **1** (0.3mM) in different concentration of HPO_4^- and the ionic strength was maintained by adding $NaClO_4$.

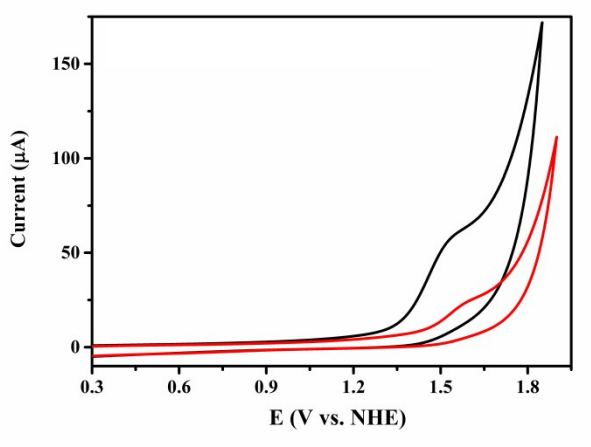

Figure S16: CV of complex **1** (0.2 mM) in pH 8 0.1 M phosphate buffer with (black line) and without KCl (red line).

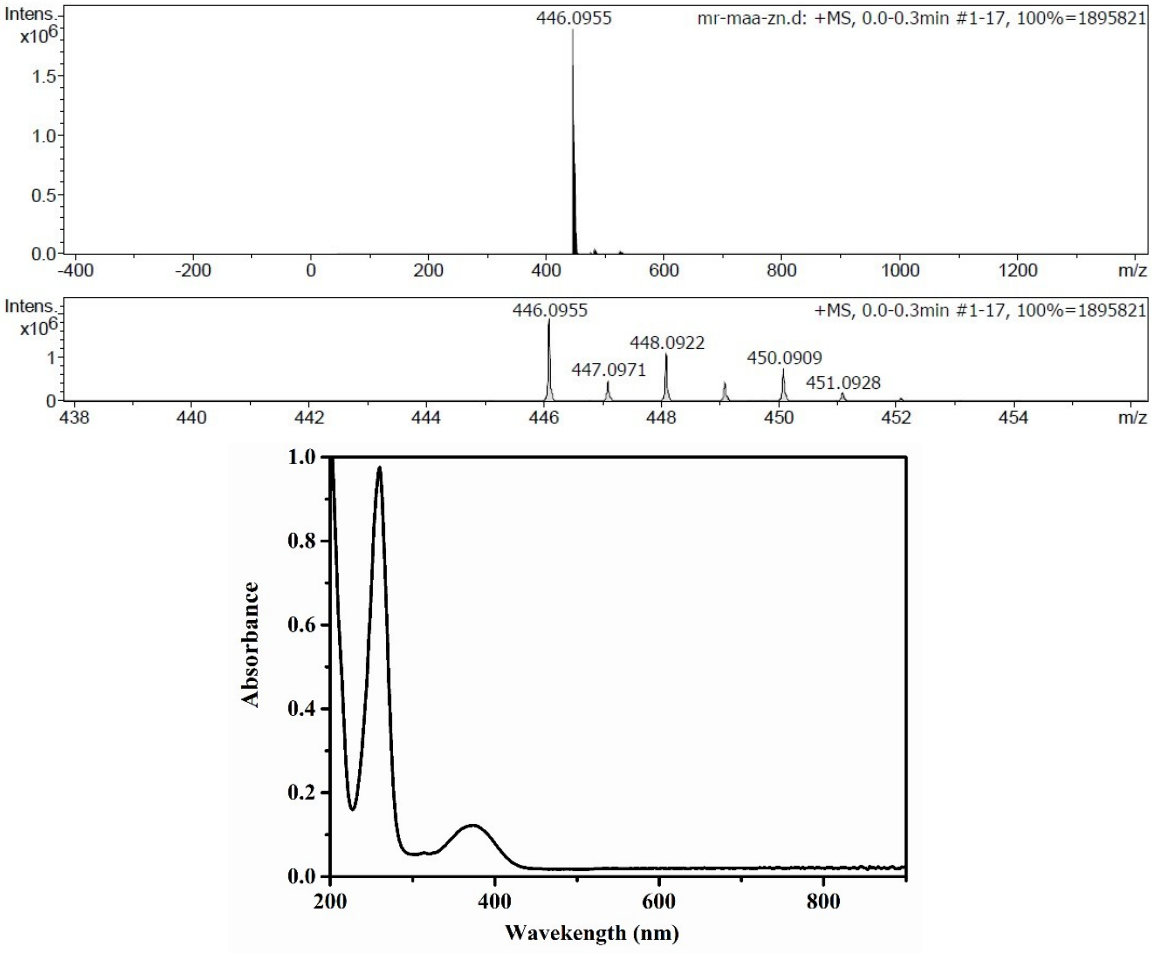

Figure S17: (top) ESI-MS spectra of $[Zn(dpaq)]^+$ in acetonitrile. (bottom) UV-Vis spectra of the Zn(complex) (25 μM) in acetonitrile.

Reference:

1. Y. Li, W. Zhou, H. Wang, L. Xie, Y. Liang, F. Wei, J. C. Idrobo, S. J. Pennycook, H. Dai, *Nature Nanotech.* **2012**, *7*, 394-400.
2. C. Costentin, S. Drouet, M. Robert and J.-M. Savéant, *Journal of the American Chemical Society*, **2012**, 134, 11235-11242.
3. R. S. Nicholson and I. Shain, *Analytical Chemistry*, **1964**, 36, 706-723.